Materials Research Proceedings 41 (2024) 316-324 https://doi.org/10.21741/9781644903131-36

Experimental and numerical study of heat transfer on an industrial FFF printer: Application to PEEK

BENARBIA Adel[1,2,a *], SOBOTKA Vincent[1,b], BOYARD Nicolas[1,c] and ROUA Christophe[2,d]

[1]Nantes Université, CNRS, LTEN, UMR 6607, F-44000 Nantes, France

[2]Cogit Composites company, 9117 rue des Vignerons 18390 Saint-Germain-du-Puy, France

[a]adel.benarbia@univ-nantes.fr, [b]vincent.sobotka@univ-nantes.fr, [c]nicolas.boyard@univ-nantes.fr, [d]christophe.roua@cogit-composites.com

Keywords: Fused Filament Fabrication (FFF), Heat Transfer, Printer Characterization, Crystallization, Semicrystalline Polymer, Experimental Study, Numerical Simulation

Abstract. The FFF process is one of the most widely used additive manufacturing processes for shaping thermoplastic polymers. The recent development of industrial printers equipped with high-temperature ovens has made it possible to print high-performance thermoplastics from the PAEK family for applications in the aerospace, medical and other industries. Numerous studies have shown that thermal history is a key factor to improve the mechanical properties of printed parts. Nevertheless, the uniformity of mechanical properties of printed parts is generally poor and highly dependent on the homogeneity of the thermal oven used, which, to our knowledge, has never been properly characterized. For semi-crystalline polymers, the thermal driven crystallization process is also a key factor in adhesion. However, the coupling between phase transformation and heat transfer is often neglected in numerical modelling and its influence has not yet been clearly demonstrated. In this work, we will carry out a preliminary characterization of the printer by measuring air velocity and temperature gradients over the whole printing zone. Secondly, the comparison between simulation and experimental measurements will show the importance of correctly predicting crystallization kinetics to obtain more accurate predictions.

Introduction

In recent years, additive manufacturing has been the subject of many studies, regardless of the type of technology. The Fused Filament Fabrication (FFF) process being the most widespread, a great deal of attention has been paid to it. It is one of the most affordable additive manufacturing technologies which is simple and with a fast manufacturing speed. Nevertheless, one of the notable limitations of the additive manufacturing process is the decrease of the mechanical properties of the produced parts, compared to conventional processes like injection molding. These mechanical properties are low in the direction normal to the interfaces, resulting in high anisotropic properties [1]. Such behaviour is the consequence of the presence of porosities and the low interfacial strength between filaments. For this reason, a lot of researches have been performed to improve the quality of the parts manufactured with this process [1,2]. Industrial manufacturers have also developed large-scale printers equipped with high-temperature ovens to print PEAKs such as Polyetheretherketone (PEEK) (Figure 1) [3].

In the FFF process, the polymer material is passed through an extruder consisting of a heating system and a nozzle to form the filament. The melted filament is then deposited along a specific trajectory to produce a layer. The platform is successively lowered along the z axis by an increment equal to the layer thickness, allowing the process to proceed layer by layer until the desired geometry is achieved.

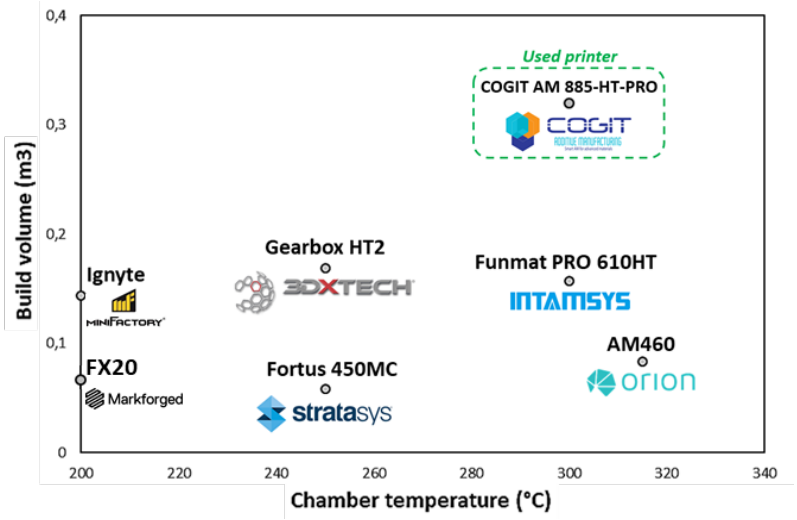

Figure 1 - Comparison of the printing volume of PEEK printers according to their chamber temperature. Only PEEK printers with a chamber temperature above 200°C and a volume greater than 0.05m^3 are shown.

Process adhesion takes place in several steps. During the deposition, intimate contact occurs and interfaces develop with the other filaments. This phenomenon called coalescence is followed by the healing process where polymer chains diffuse through the interfaces in order to create a real molecular bond with the others filaments [4]. These adhesion mechanisms are only possible if the molecular chains present at the interfaces have sufficient mobility [5]. Molecular mobility is governed by the thermodynamic state of polymers, which explains the significant influence of thermal history on adhesion kinetics [6].

Studies were conducted to predict the thermal history of the FFF process [4,7]. From these works, numerical Finite Element Method (FEM) models were developed and showed good agreement with experimental tests in the case of amorphous polymers. However, for semi-crystalline polymers, endothermal and exothermal phase transformation reactions are rarely taken into account and their influence has not yet been demonstrated numerically or experimentally.

Heat transfer being a primary importance on the quality of the printed parts, a good knowledge of thermal behavior of heated chamber is required. 3D printing ovens, have most of the time a poorly insulating upper wall due to the mobility function and require thus air circulation to prevent vertical thermal stratification. The use of a rotating fan ensures a uniform temperature, but can also result in a highly variable airflow. To avoid this, air curtain systems have been developed and integrated to ensure a constant, homogeneous and linear air flow over the upper part of the oven. However, multiple circulation systems and poorly insulated upper wall generally lead to significant temperature fluctuations, particularly on large scale printer.

As heat exchange between the air and the printed part has a major influence on heat transfer, a preliminary characterisation of the printer was carried out in order to determine the thermal homogeneity of the printing environment. This characterisation is necessary in order to define whether the temperature and the convective heat transfer coefficient can be considered constant over the whole printing volume for the numerical modelling. *In situ* thermal monitoring of the process was also carried out to measure the thermal history depending on process parameters. The experimental measurements were compared with the numerical simulation in order to validate the model and show the influence of the energy released during the crystallization on heat transfer.

Experimental section

Industrial Printer

The tests were carried out on the COGIT AM 885-HT-PRO FFF industrial printer developed by COGIT AM (Figure 2). The printer is a Cartesian type machine with a printing volume of 800x800x500 mm^3. The printer consists of an extruder that deposits the filament on a bed in an oven with a volume of 1.5m3. The oven has been dimensioned to reach 300°C in the whole chamber. The extruder moves along the X and Y axis and the bed is lowered along the Z axis. The COGIT 885-HT-PRO is a flexible and open machine. It has been designed to easily implement complementary modules for research purposes, such as in-situ instrumentation systems (optical and thermal cameras), pellet extruders, local heating (infrared lamps and laser), gripping and placement systems, etc.

Figure 2 – COGIT AM 885-HT-PRO printer.

Air flow rate printer characterization

In order to determine whether the convective heat transfer coefficient can be considered independent of the printing position, the air velocity was measured over the whole printing surface. The air circulation system of the COGIT AM 885-HT-PRO consists of two fans positioned along the height of the oven. (areas 1 and 2 in Figure 3). The air curtain (area 3 in Figure 3) is positioned above the air circulation system at 90° to the circulation direction. The flow rate of the three mixing systems can be controlled separately. In this study, the three circulation systems were controlled at a constant flow rate. The air curtain is positioned at the height of the printing nozzle so that it is effective over the first fifty millimeters printed. As convective heat transfer between the air and the filaments has an influence on the thermal history only for the first printed layers, only the air curtain flow was characterized. Measurements were therefore taken at a fixed altitude Z=0mm.

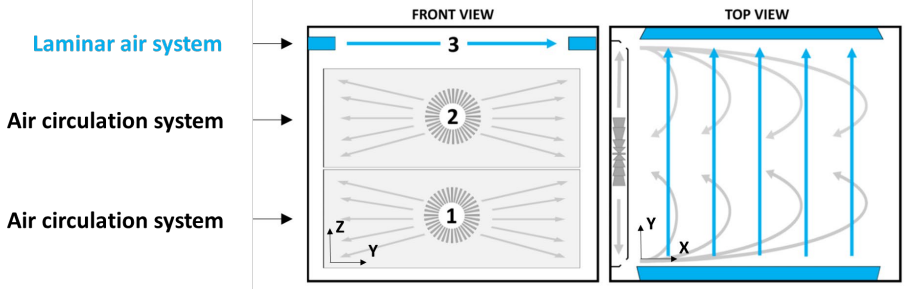

Figure 3 - Schematics of the COGIT AM 885-HT-PRO circulation air systems.

The air velocity was characterized with a hot wire anemometer positioned on the tool holder instead of the extruder and then moved along the XY axes. The anemometer is moved along a specified path using a back and forth motion to map the air velocity over the full print area 800x800mm (Figure 4). The anemometer head is positioned at the same height as the nozzle to characterize the air curtain at Z=0mm.

The anemometer travel speed is 10mm/s and the sampling rate is 2Hz. The displacement speed is assumed to be slow enough to not disturb the airflow or the measurement. The anemometer is capable of measuring over a range of 0.1 to 30 m/s with an accuracy of ± 3% of the measurement. The tests were carried out at room temperature, assuming that the influence of temperature on airflow is negligible. The measurements will therefore be considered valid regardless of the printing temperature. The recording of the speed is triggered simultaneously with the anemometer movement in order to associate each measurement with a position in the XY plane. A 2D linear

interpolation of the measurements was carried out to obtain the airflow map of the XY plane at height of Z=0mm (Figure 4).

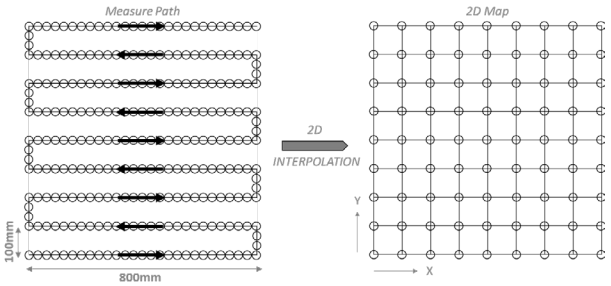

Figure 4 - Diagram of the tool holder trajectory in the XY plane and 2D interpolation to obtain a 2D map.

Temperature oven characterization

3D printing ovens have a poorly insulating upper wall due to the mobility function, so air circulation is necessary to avoid vertical temperature gradients. Despite the correct air circulation system, it is necessary to have a uniform temperature distribution throughout the printing volume to ensure uniform mechanical and geometric quality of the parts. The air temperature was therefore characterized over the entire 800x800x500mm printing volume. As the process window for PEEK is between 200 and 300°C, the temperature measurements were taken in the middle of the range at a fixed setpoint of 250°C.

Air temperature was measured using class 1 type J thermocouples capable of measuring from -40 to 600°C with an accuracy of ± 1.5°C. The thermocouples are made up of two 300µm diameter conductors giving them a short response time of 0.7s in air. The thermocouples are connected to an acquisition unit (Graphtec GL220) capable of reading and recording up to 10 thermocouples simultaneously with a sampling time of 5Hz.

In order to determine the temperature evolution as a function of height, several thermocouples were positioned at different levels on a support. The discretization of the measurement points was defined in such a way as to detect thermal gradients, particularly in the upper part of the oven. 9 thermocouples were therefore positioned at 0, 25, 50, 70, 100, 125, 250, 375 and 500mm in order to completely cover the printing height (Figure 5).

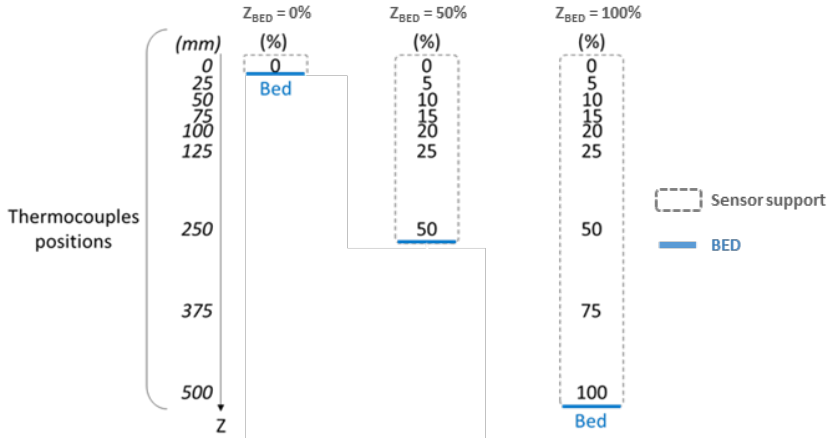

Figure 5 - Representation of the thermocouple positions on the support along the Z axis for 3 different configurations.

The printing bed, even if it is not heated, can have an influence on the air flow and therefore on the heating system. In order to take this influence into account, the bed was positioned at 3 different altitudes 0, 50 and 100% of the Z axis, i.e. 0, 250 and 500mm. In this way, when the bed is at an altitude of 0mm, only 1 thermocouple is present on the support. When the bed is at 50%, 7

thermocouples are present to map the enclosure. Finally, when the bed is at Z=100%, all thermocouples are used on the sensor support, as shown in the figure.

In the same way as for the airflow characterization presented previously, the thermocouple support is fixed to the tool holder instead of the extruder. The support is moved in the same path along XY in order to measure the temperature over the whole printing area. The same interpolation method is used to obtain the 2D temperature map. As a result, 2D temperature mapping is obtained at each altitude where a sensor is positioned. For example, when the bed is at 100% height, we obtain 9 2D maps in the XY plane at altitudes of 0, 25, 50, 70, 100, 125, 250, 375 and 500mm.

The thermocouples are thermally insulated from its support by a silicone-coated glass sheath and positioned so that the weld point is only in contact with the air. The displacement speed of 10mm/s is considered to have no effect on the measurement, considering the fast response time of the sensor and the small temperature variations measured. As the thermocouples were installed before heating the printing enclosure, a sensor positioning accuracy along the Z axis of ± 2mm can be considered, taking into account the thermal expansion of the sensor support from 25 to 250°C.

Thermal history measurement of printed part

The thermal history of printed filaments is carried out using an infrared thermal camera positioned inside the printing enclosure (Figure 6). The infrared camera has a measurement range between 150 and 900°C and detects wavelengths from 8 to 14 µm. The emissivity of PEEK has been measured and can be considered constant over the 8-14 µm wavelength range with a value of ε = 0.92. The thermal camera is mounted on the printing bed at a distance of 100mm from the part, where the pixel size corresponds to a surface of 90 x 90 μm^2.

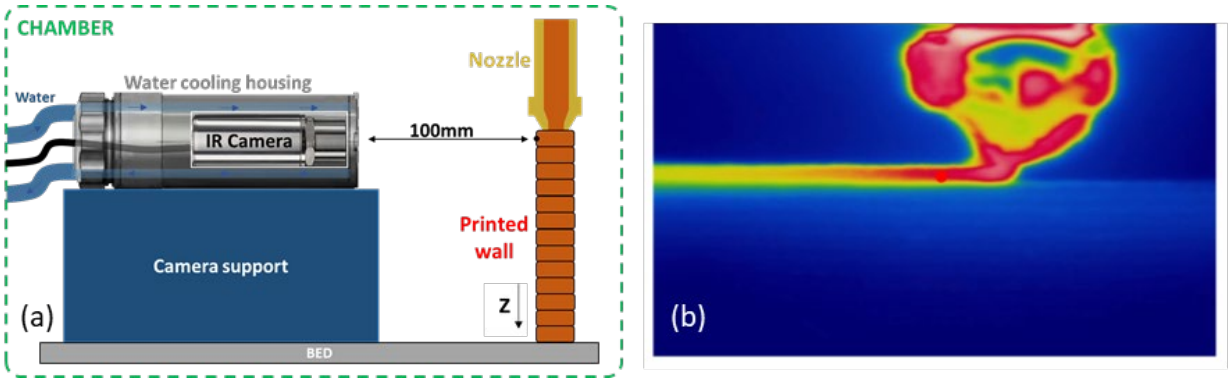

Figure 6 – Diagram of the bench used to measure the thermal history of printed filament (a). Thermal image obtained (b).

In order to take into account, the effects of environmental radiation on the measurement, the camera was calibrated beforehand. The calibration consisted in comparing temperatures between the camera and a thermocouple welded to the surface of the printed part. Temperature steps were taken from 150 to 250°C every 10°C to obtain the correction curve that was applied to the thermal measurements. The infrared camera is positioned in a water cooling housing to keep it below its maximum operating temperature.

The infrared images are acquired at 80Hz, allowing the cooling of the filament over time to be correctly observed. The thermal history of 5 filaments is measured between the 20^{th} and 30^{th} filaments where there is no further influence of the printing bed. The average of the 5 measurements is calculated and taken as a reference for comparison with the simulation results.

The prints were performed in the centre of the bed at a printing speed of 20mm/s. The walls consisted of a single filament across the width and measured 40mm high and 50mm long. The deposited and simulated filament is 1mm wide with a layer thickness of 0.5mm, so 5 pixels of the

infrared camera can measure the temperature along this direction. The deposition time between each layer is 12.2s. These conditions and printing geometry are commonly used for PEEK.

Modeling section

In this work, heat transfers and phase transformations are implemented in a coupled multiphysics model. The numerical solving was performed with COMSOL® FEM software on a 2D model. A 30 filament high wall was simulated in one step calculation. The thermal history is recorded on the 25th filament at mid-height on the outer surface in contact with the chamber air. The reading is taken at the same point where the temperature is measured with the infrared camera, so that the results can be compared. Model parameters such as layer thickness, printing speed, nozzle temperature are identical to the real process.

The thermal model is represented in Figure 7 in which we solve the energy equation coupled to crystallization and melting. The source term in the energy equation depends on ΔH, the crystallization and melting enthalpies and α, the crystalline degree. [8]. For more information on the multiphysic model, please refer to [9].

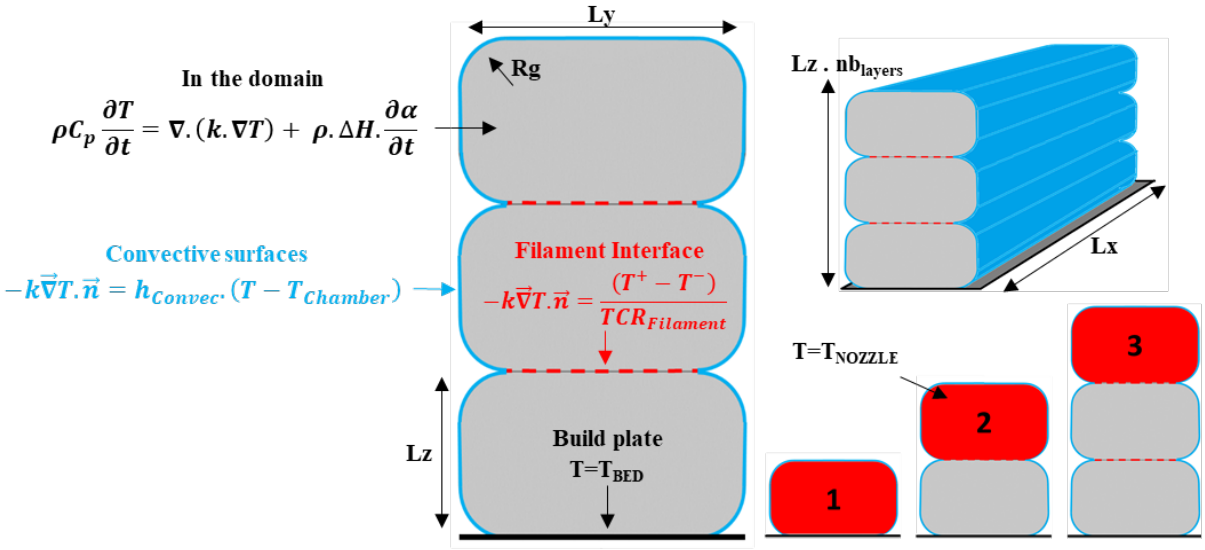

Figure 7 - Schematic representation of the numerical model.

Results and discussion

The air velocity norm map of the industrial printer COGIT AM 885-HT-PRO is shown in Figure 8.a. The velocity values are centered around 0.85 m/s with a standard deviation of 0.13 m/s (Figure 8.b). The velocity of the area was averaged along the X and Y directions shown in Figure 8.c and Figure 8.d respectively. It can be seen that for positions close to Y=0mm, the air velocity is greater to 1.8m/s. This is due to the proximity of the air curtain outlet. In Figure 8.a or Figure 8.d, a slight slowing of the air velocity is observed at both ends of the X axis (X<50mm and X>750mm). This is due to the edge effects of the air curtain which is positioned along the X axis. Overall, the heat transfer coefficient will be considered constant for positions of Y greater than 50mm and X between 50 and 750mm as indicated by the green rectangle in Figure 8.a.

Materials Research Proceedings 41 (2024) 316-324 https://doi.org/10.21741/9781644903131-36

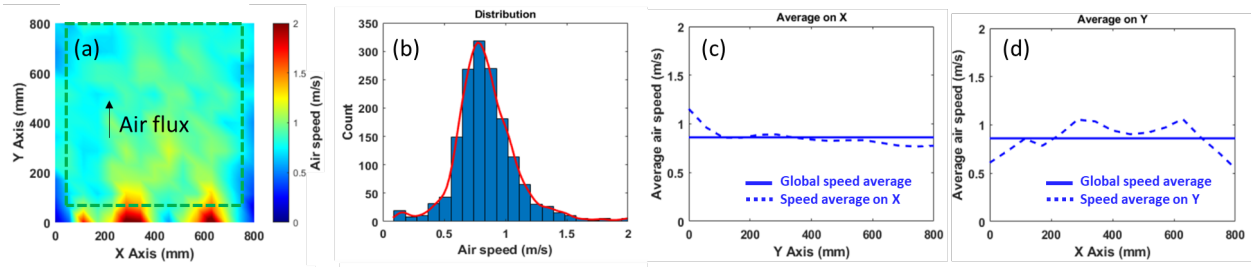

Figure 8 - Air velocity norm map (a), measure distribution (b), average air speed along Y (c) and X (d) axis.

The thermal measurements of the printer are shown in Figure 9 for 3 different bed positions. For each configuration, a 3D map is defined where each plane corresponds to the position of a thermocouple that has been moved along XY. No real influence of the bed position could be observed.

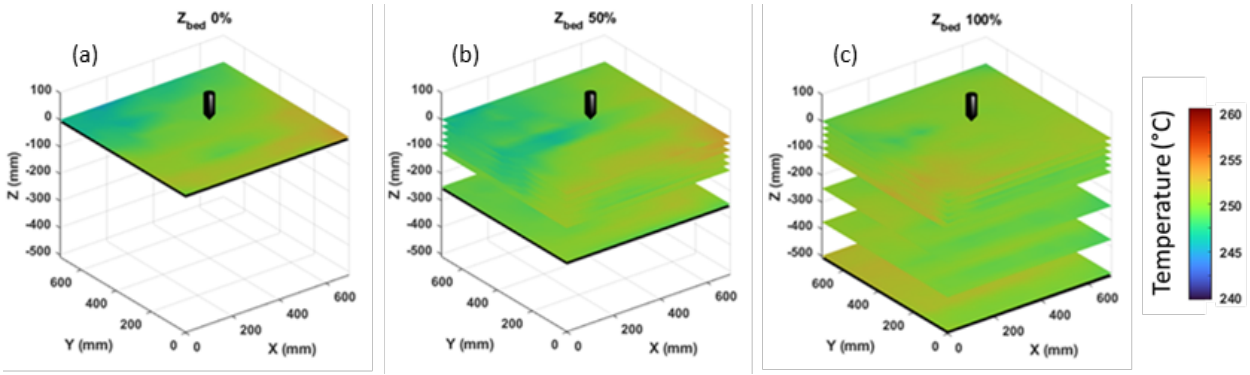

Figure 9 - Thermal 3D map for 3 different bed height : 0% (a), 50% (b) and 100% (c). The bed and nozzle are shown in black as spatial references.

In order to get the most out of the results, statistical calculations were carried out for each measurement plan. In Figure 10, the mean, standard deviation, minimum and maximum recorded temperatures were plotted for each measured height in the form of a whisker diagram for configuration Z_{BED} = 100%. The results show a high degree of thermal stability in the chamber, with relatively low standard deviations of less than 1°C. It can also be seen that the standard deviation decreases with increasing Z, which means that the lower part of the oven is more homogeneous than the upper part. Over the full printing volume, the minimum temperature detected is 245°C and the maximum is 255°C. The machine's oven is therefore capable of keeping the chamber at 250±5°C over a volume of 800x800x500mm^3.

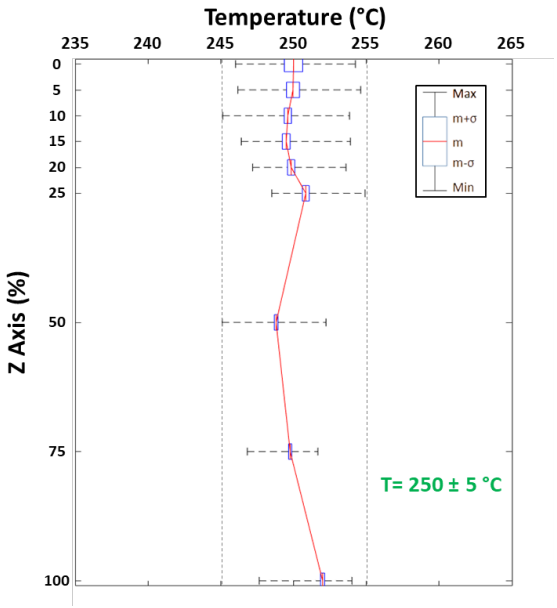

Figure 10 – Statistic data evolution along Z axis. Average temperature (—), standard deviation (—), minimum and maximum recorded temperatures (--) for each XY measured height map.

3 different thermal cases were experimentally measured and numerically estimated. The thermal cases were carried out under the same conditions with only the chamber temperature changing: 180, 200 and 220°C. The superposition of the experimental measurements made with the pixel located in the middle of the layer thickness and the numerical results of the single-walls is shown in the Figure 11. It can be seen that the numerical modelling seems to be in good agreement with the experimental results.

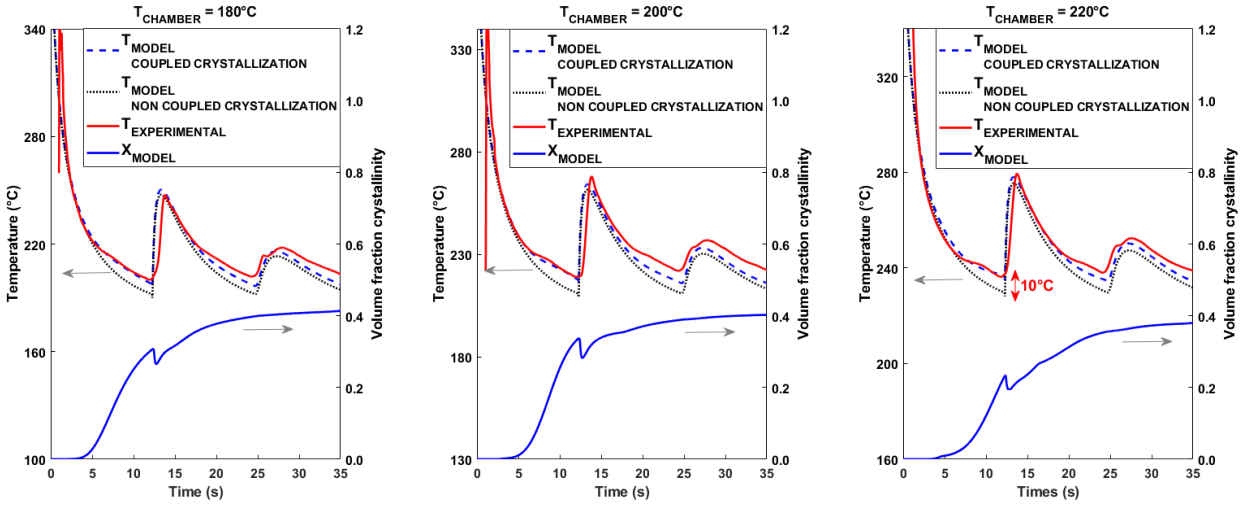

Figure 11 – Thermal history experimentally measured (—), numerically computed with (- -) and without (· · ·) crystallization coupling, on left axis. Volume fraction crystallinity evolution (—), on right axis.

During cooling of the first deposited filament, the experimental measurements (red solid line) show an abrupt change in cooling rate after 4, 6 and 8 seconds for 180, 200 and 220°C respectively. This behaviour change is also predicted by the numerical simulation (blue dashed lines) and corresponds to the start of crystallization. Indeed, the enthalpy produced during crystallization appears to have a non-negligible effect on the thermal history of the material. In order to show the influence of crystallization enthalpy, the thermal simulation was simulated without crystallization

coupling (black dotted lines). It can be seen that as long as crystallization has not begun, the simulations with and without the coupling are perfectly superimposed. The simulation without the coupling to crystallization can underestimate the temperature with an error of up to 10K.

Conclusion

The thermal environment of a high-temperature large scale industrial printer was characterized experimentally. Firstly, the air flow rate of the air curtain was measured and a good homogeneity of the velocity was observed over the entire printing surface, with the exception of the boundary. In addition, the air temperature was characterized in 3 dimensions over the full printing volume, taking into account the presence of the printing bed. No influence of the printing bed on temperature was observed. No significant fluctuations were also observed, with chamber stability of ± 5°C at a set temperature of 250°C.

The thermal history of printed walls was measured experimentally at different chamber temperatures on the high-temperature industrial printer. Good agreement between experimental and numerical results confirms the validity of the model. The abrupt change of the surface filament experimental temperature observed during cooling was correctly predicted by the model and demonstrated the importance of taking account of the enthalpies of crystallization in the heat equation.

In future work, adhesion measurements will be carried out experimentally and compared with the predictions of the multiphysics model, which takes into account a crystallization-coupled adhesion model.

References

[1] Popescu D, Zapciu A, Amza C, Baciu F, Marinescu R. FDM process parameters influence over the mechanical properties of polymer specimens: A review. Polymer Testing 2018;69:157–66. https://doi.org/10.1016/j.polymertesting.2018.05.020

[2] Lepoivre A, Boyard N, Levy A, Sobotka V. Heat Transfer and Adhesion Study for the FFF Additive Manufacturing Process. Procedia Manufacturing 2020;47:948–55. https://doi.org/10.1016/j.promfg.2020.04.291

[3] PEEK 3D PRINTING – The ultimade guide. All3dp 2023. https://all3dp.com/1/peek-3d-printer/

[4] Xu D, Zhang Y, Pigeonneau F. Thermal analysis of the fused filament fabrication printing process: Experimental and numerical investigations. Int J Mater Form 2021;14:763–76. https://doi.org/10.1007/s12289-020-01591-8

[5] Barocio E, Brenken B, Favaloro A, Pipes RB. Interlayer fusion bonding of semi-crystalline polymer composites in extrusion deposition additive manufacturing. Composites Science and Technology 2022:109334. https://doi.org/10.1016/j.compscitech.2022.109334

[6] Lo C-T, Laabs FC, Narasimhan B. Interfacial adhesion mechanisms in incompatible semicrystalline polymer systems. J Polym Sci B Polym Phys 2004;42:2667–79. https://doi.org/10.1002/polb.20148

[7] Costa SF, Duarte FM, Covas JA. Estimation of filament temperature and adhesion development in fused deposition techniques. Journal of Materials Processing Technology 2017;245:167–79. https://doi.org/10.1016/j.jmatprotec.2017.02.026

[8] Zanjanijam AR, Major I, Lyons JG, Lafont U, Devine DM. Fused Filament Fabrication of PEEK: A Review of Process-Structure-Property Relationships. Polymers 2020;12:1665. https://doi.org/10.3390/polym12081665

[9] Benarbia A, Sobotka V, Boyard N, Roua C. Fused filament fabrication: Numerical adhesion modeling suitable for semicrystalline polymers, 2023, p. 139–48. https://doi.org/10.21741/9781644902479-16.